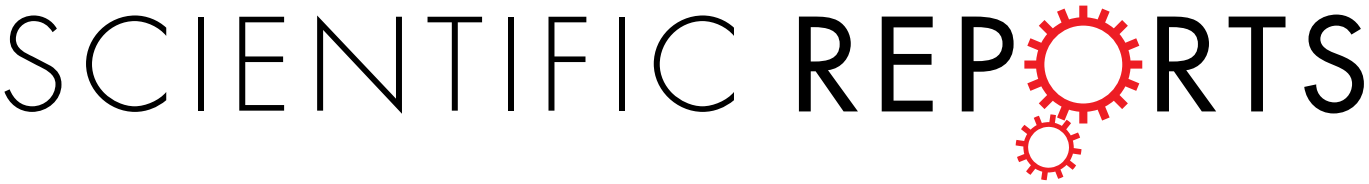

OPEN

Phonon-mediated high-T_c superconductivity in hole-doped diamond-like crystalline hydrocarbon

Received: 31 October 2016
Accepted: 16 March 2017
Published online: 03 May 2017

Chao-Sheng Lian[1], Jian-Tao Wang[1,2], Wenhui Duan[3] & Changfeng Chen[4]

We here predict by *ab initio* calculations phonon-mediated high-T_c superconductivity in hole-doped diamond-like cubic crystalline hydrocarbon K_4-CH (space group $I2_13$). This material possesses three key properties: (i) an all-sp^3 covalent carbon framework that produces high-frequency phonon modes, (ii) a steep-rising electronic density of states near the top of the valence band, and (iii) a Fermi level that lies in the σ-band, allowing for a strong coupling with the C-C bond-stretching modes. The simultaneous presence of these properties generates remarkably high superconducting transition temperatures above 80 K at an experimentally accessible hole doping level of only a few percent. These results identify a new extraordinary electron-phonon superconductor and pave the way for further exploration of this novel superconducting covalent metal.

Covalent metals are fascinating materials derived from doping selected semiconductors or insulators[1]. The strong directional bonding in these crystals produces high-frequency phonon modes that, when favorably coupled to charge carriers, are conducive to generating superconductivity at a high transition temperature T_c. The prospects of finding light-element-based electron-phonon high-T_c superconductors have attracted reinvigorated research efforts in recent years[2–5]. Prominent among covalent metals are the carbon-based systems, whose structural versatility can be explored to tune the electronic, lattice, and electron-lattice coupling properties to optimize T_c. Graphite and fullerene are prototypical sp^2-bonded carbon structures that become superconducting when doped with alkali or alkali-earth metals; examples include CaC_6 with $T_c = 11.5$ K[6,7], and $RbCs_2C_{60}$ with $T_c = 33$ K[8,9] Superconductivity has also been observed in alkali-metal-doped aromatic hydrocarbons, e.g., K_3 picene with $T_c = 18$ K[10]. Meanwhile, diamond is the archetype of sp^3-bonded carbon structures that turns into a superconductor with boron substitution. In contrast to the sp^2-bonded structures with π electrons as the main charge carriers[8,10], boron-doped diamond has holes injected into the σ states that respond sensitively to the strong bond-stretching phonon modes[11]. A similar electron-phonon coupling in the σ-band of MgB_2 produced a T_c of 39 K[12,13]. Doped diamond, however, has much lower T_c values in the range of 4 to 11 K at the boron concentration of 2.8 to 5%[14–16].

According to the Bardeen-Cooper-Schrieffer theory of superconductivity[17], achieving high T_c requires the simultaneous presence of high-frequency phonon modes, a large electron-phonon coupling, and a high electronic density of states (DOS) at the Fermi level (N_F). These conditions are only partially met in most previously studied systems. For example, the sp^2-bonded carbon structures have high N_F values but only moderate to low electron-phonon coupling, while the sp^3-bonded diamond has high-frequency phonon modes and strong electron-phonon coupling but low N_F values[2,18]. It has been predicted that diamond could reach higher T_c of up to 55 K with a 30% boron doping[19], but such a high doping level is hard to achieve experimentally[20]. Theoretical efforts also explored materials with narrow electronic bands or reduced dimensionality to enhance N_F and obtained promising results, although material synthesis and stabilization remain challenging[21,22].

[1]Beijing National Laboratory for Condensed Matter Physics, Institute of Physics, Chinese Academy of Sciences, Beijing, 100190, China. [2]School of Physics, University of Chinese Academy of Sciences, Beijing, 100049, China. [3]Department of Physics and State Key Laboratory of Low-Dimensional Quantum Physics, Tsinghua University, Beijing, 100084, China. [4]Department of Physics and High Pressure Science and Engineering Center, University of Nevada, Las Vegas, Nevada, 89154, USA. Correspondence and requests for materials should be addressed to J.-T.W. (email: wjt@aphy.iphy.ac.cn)

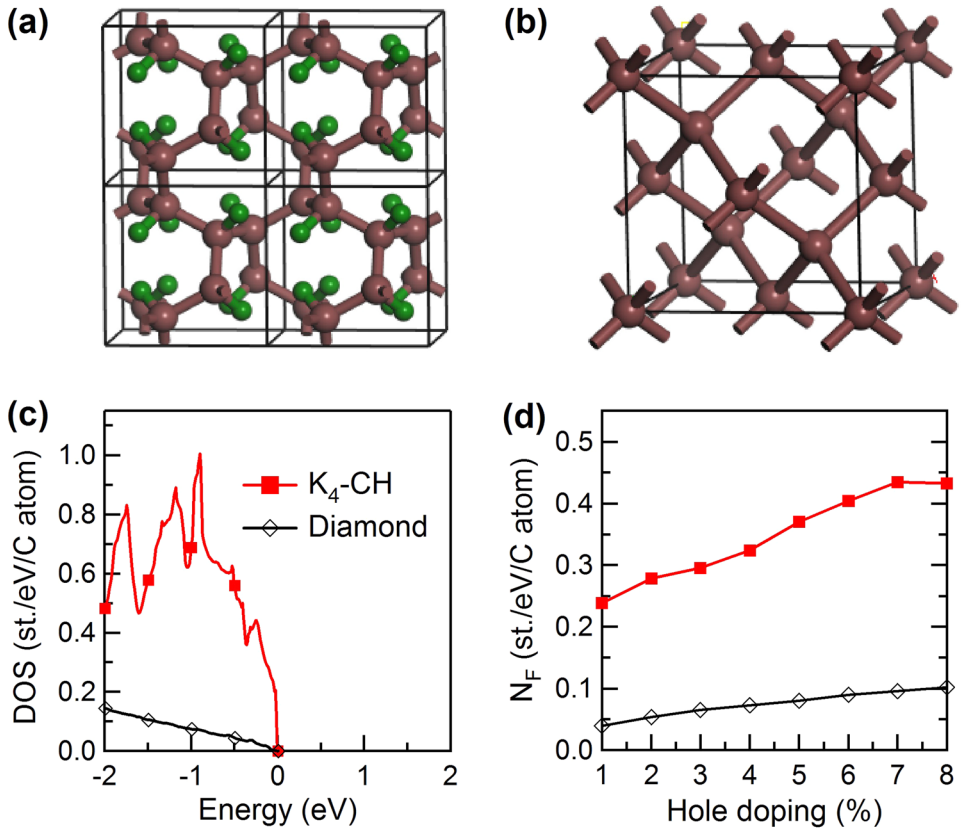

Figure 1. (**a**) Crystal structure of K_4-CH ($I2_1/3$), in comparison with that of (**b**) diamond ($Fd\bar{3}m$). Large brown and small olive spheres represent the C and H atoms, respectively. The atomic Wyckoff positions are 8a (0.8384, 0.6616, 0.3384) C and 8a (0.1893, 0.3107, 0.6893) H for K_4-CH. (**c**) Electronic density of states (DOS) and (**d**) N_F as a function of hole doping for K_4-CH and diamond. The top of the valence bands is set as energy zero.

In this paper, we identify by *ab initio* calculations phonon-mediated high-T_c superconductivity in hole-doped cubic crystalline hydrocarbon K_4-CH[23] (space group $I2_1/3$, named after the K_4 carbon[24]). This structure comprises a strong sp^3-bonded carbon framework as in diamond [see Fig. 1(a)], which produces high-frequency phonon modes. Moreover, it also possesses a quickly rising electronic DOS near the top of the valence σ-band, allowing for a strong electron-phonon coupling. The presence of all three key properties required for phonon-mediated high-T_c superconductivity produces T_c values above 80 K in K_4-CH at an experimentally accessible hole doping level of a few percent. These results promise to stimulate efforts for synthesis and further exploration of this novel superconducting covalent metal.

Results

The structural detail of K_4-CH is schematically depicted in Fig. 1(a). This hydrocarbon crystallizes in a body-centered cubic structure with equilibrium lattice parameter $a = 4.250$ Å. The calculated C-C bond length for K_4-CH is 1.566 Å, close to 1.532 Å for diamond [Fig. 1(b)], indicating the saturated nature of the sp^3 carbon bonding in forming the three-dimensional (3D) covalent framework. Figure 1(c) shows the calculated electronic DOS for diamond and K_4-CH. In diamond, the DOS increases slowly into the valence band. In stark contrast, in K_4-CH, the DOS rises steeply from the valence band edge, reaching high values at low doping levels. Results in Fig. 1(d) show that at 3% hole doping the value of N_F for K_4-CH reaches 0.30 states/eV/C, which are almost five times as high as the 0.065 states/eV/C for diamond. Such a significant DOS enhancement in the hydrocarbon is ascribed to the much smaller band dispersion in the proximity of the valence bands compared to diamond (see Fig. S2 in Supplementary Information).

The phonon dispersion ($\omega_{q\nu}$) and phonon density of states (PHDOS) calculated for pristine and hole-doped K_4-CH are shown in Fig. 2. For pristine hydrocarbon, no imaginary phonon frequencies are found in the whole Brillouin zone, indicating its dynamical stability. In the presence of hole doping, the calculated optical phonon dispersions exhibit an obvious softening near the zone center, similar to the cases of doped diamond[18] and graphane[22].

To gain insights into the influence of the optical phonon modes that dominate the EPC in hole-doped hydrocarbon, we evaluate the electron-phonon interaction $\lambda_{q\nu}$ for a phonon mode ν with momentum $\mathbf{q}$[25]:

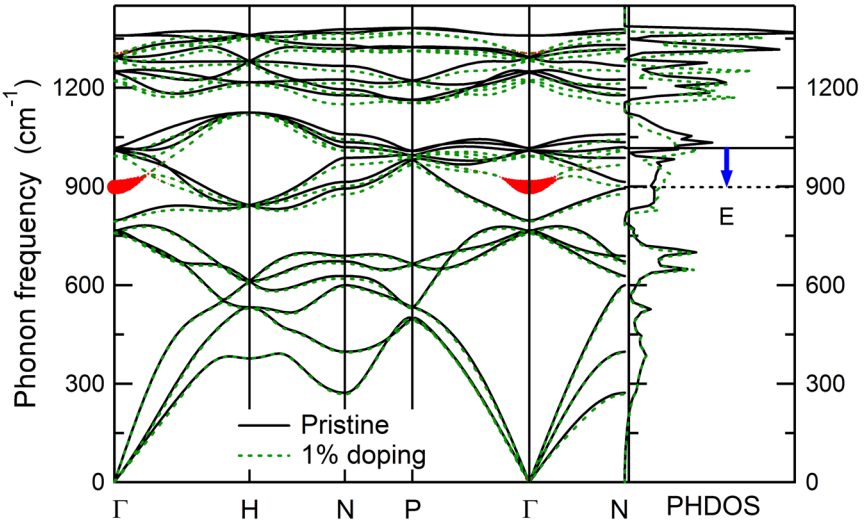

Figure 2. Phonon dispersion and PHDOS of pristine and 1% hole-doped K_4-CH. The thickness of the red curves denotes the mode EPC strength $\lambda_{\mathbf{q}\nu}$ [Eq. (1)]. The softening of the optical zone-center modes is indicated by the blue arrow.

$$\lambda_{\mathbf{q}\nu} = \frac{4}{\omega_{\mathbf{q}\nu} N_F N_k} \sum_{\mathbf{k},n,m} |g^{\nu}_{\mathbf{k}n,\mathbf{k}+\mathbf{q}m}|^2 \delta(\epsilon_{\mathbf{k}n}) \delta(\epsilon_{\mathbf{k}+\mathbf{q}m}), \tag{1}$$

where $\omega_{\mathbf{q}\nu}$ is the phonon frequency, $\epsilon_{\mathbf{k}n}$ is the Kohn-Sham energy, and $g^{\nu}_{\mathbf{k}n,\mathbf{k}+\mathbf{q}m}$ represents the electron-phonon matrix element. It is seen from Fig. 2 that for K_4-CH the two-fold degenerate optical E modes at Γ with the largest EPC are softened by 120 cm^{-1} at 1% doping. By inspecting the calculated vibrational pattern of the softened modes [see the insets of Fig. 3(a)], we find that these transverse optical (TO) zone-center phonon modes correspond to the C-C bond stretching modes, which couple considerably to the holes at the top of the σ-bonding valence bands. Furthermore, the softening of the TO C-C stretching modes (120 cm^{-1} at 1% doping) is comparable to the 138 cm^{-1} of diamond[18] but significantly smaller than the 470 cm^{-1} of graphane[22]. This can be explained by the 3D nature of the carbon framework in K_4-CH as in diamond, which has a weaker Kohn effect that reduces the mode softening compared to 2D graphane[22]. It is noted that the high-frequency C-H stretching modes are only weakly affected by the hole doping (see Fig. S3 in Supplementary Information), suggesting their small contributions to the EPC as in doped graphane[22].

We next examine the doping induced superconductivity in the hydrocarbon. We show in Fig. 3(a) the calculated Eliashberg spectral function $\alpha^2F(\omega)$ for 1% and 3% hole-doped K_4-CH, which describes the relative contribution to the EPC by different phonon modes[25]:

$$\alpha^2F(\omega) = \frac{1}{2N_q} \sum_{\mathbf{q}\nu} \lambda_{\mathbf{q}\nu} \omega_{\mathbf{q}\nu} \delta(\omega - \omega_{\mathbf{q}\nu}). \tag{2}$$

As in doped diamond and graphane[18,22], the electron-phonon interaction here is also dominated by the coupling of the σ holes to the optical phonon modes, and only a small contribution comes from the acoustic phonon modes. There is a single dominant peak in the Eliashberg function for K_4-CH, and the peak position corresponds to the frequency of the softened TO C-C stretching mode shown in Fig. 2. As the doping increases, the main peak of $\alpha^2F(\omega)$ moves toward lower phonon frequency, reflecting further softening of the characteristic optical mode; meanwhile, the intensity of the main peak is enhanced, resulting primarily from the sharp increase in N_F [see Fig. 1(d)], which allows more electronic states at the Fermi level to couple to the phonon modes and thus increases the EPC strength ($\lambda_{\mathbf{q}\nu}$) at the higher doping level as described by Eqs (1) and (2).

Using the Eliashberg functions, we have calculated the logarithmic average phonon frequency $\omega_{log} = \exp\left[\frac{2}{\lambda}\int d\omega \alpha^2F(\omega) \ln\omega/\omega\right]$ and the EPC parameter $\lambda = 2\int d\omega \alpha^2F(\omega)/\omega$. The obtained results for hole-doped K_4-CH are presented in Fig. 3(b). Clearly, with increased hole doping ω_{log} decreases as a result of the redshift of the optical mode that dominates the EPC, while λ increases mainly due to the increasing $\alpha^2F(\omega)$. The calculated ω_{log} at 3% doping is 703 cm^{-1} in K_4-CH, smaller than the 1077 cm^{-1} in doped diamond[18]. The reduction in ω_{log} for the hydrocarbon is due to the lower frequency of the characteristic optical modes compared to diamond; they are located in the medium frequency region of the carbon framework optical modes (see Fig. 2), in contrast to diamond that possesses the highest optical zone-center phonon modes. The corresponding λ value of K_4-CH is 0.95, considerably larger than the value of 0.30 at 3% calculated for hole-doped diamond[18]. Such large λ value compensates the relatively small ω_{log} to yield large T_c value in the doped hydrocarbon (see below).

Figure 4 shows the superconducting transition temperature T_c calculated for hole-doped K_4-CH using the modified McMillan equation[26]:

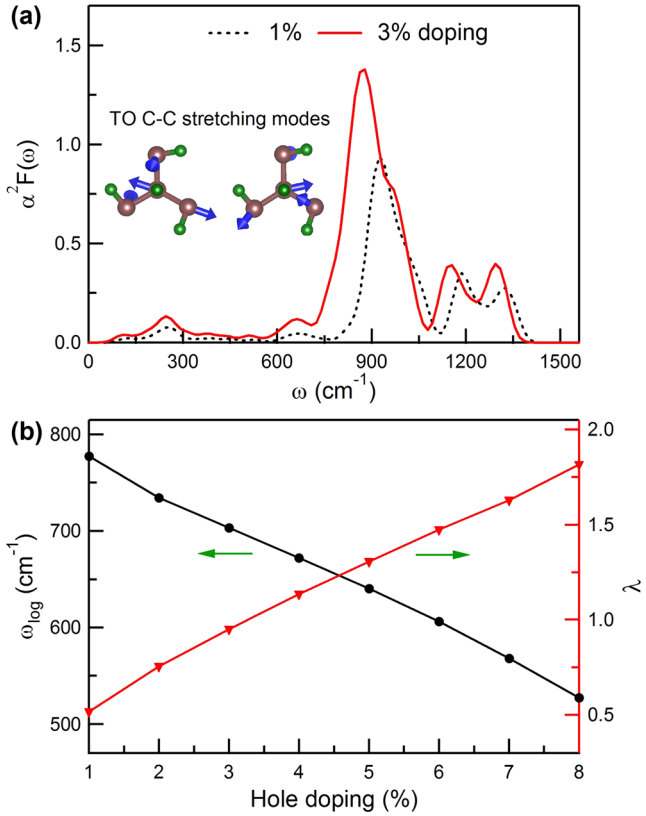

Figure 3. (**a**) Eliashberg spectral function $\alpha^2F(\omega)$ for K_4-CH at 1% (black dotted line) and 3% (red solid line) doping. (**b**) Calculated ω_{log} (black dots) and λ (red triangles) as a function of hole doping for K_4-CH. The insets in (**a**) show the characteristic TO C-C bond-stretching modes with the largest EPC contribution. The blue arrows indicate the atomic displacement patterns.

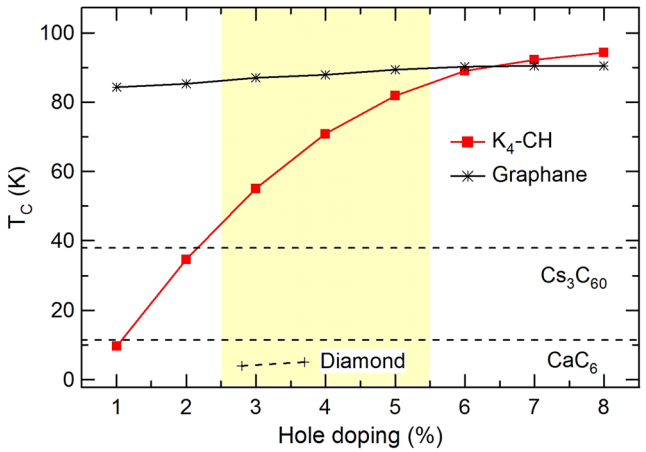

Figure 4. Calculated T_c as a function of hole doping for K_4-CH. The experimental T_c (dashed black lines) of Cs_3C_{60} (38 K[9]), CaC_6 (11.5 K[6]), and diamond (4 K at ~2.8% boron[14]; 5 K at ~3.7% boron[15]), and the theoretical T_c (solid black line) of hole-doped graphane[22] are shown for comparison. The shaded region indicates the experimentally accessible doping levels[16].

$$T_c = \frac{\omega_{log}}{1.2}\exp\left[\frac{-1.04(1+\lambda)}{\lambda - \mu^*(1+0.62\lambda)}\right], \quad (3)$$

with a screened Coulomb pseudopotential $\mu^* = 0.13$ (a typical value falling in the range 0.10–0.15 for most carbon-based materials[27–29]). It is seen that T_c increases with rising hole doping. At 3% doping, the calculated T_c is 55.1 K in K_4-CH, which is significantly larger than the T_c of 4–5 K in boron-doped diamond at comparable doping

levels[14, 15]. More remarkably, K_4-CH exhibits very high T_c values above 80 K at 5% doping and becomes competitive with the previously studied hole-doped graphane[22]. It is important that such large T_c values are achieved at the experimentally accessible low doping levels, making it feasible to realize phonon-mediated high-T_c superconductivity in this hydrocarbon.

We now comment on the synthesis and doping of the hydrocarbon studied here. Superconducting boron-doped diamond was first produced under high-pressure and high-temperature conditions[14]. Experimental evidence has shown pressure-induced polymerization of acetylene or benzene into saturated CH structures[30, 31], and this method is promising for synthesizing the sp^3-bonded hydrocarbon superconductor through high-pressure treatments of the molecular precursors with the incorporation of boron hydrides. An alternative approach is the chemical vapor deposition growth of boron-doped CH films, which has been widely used in preparing diamond-like CH films from different precursors[32, 33]. Compared with the high-pressure synthesis, growing the superconducting doped hydrocarbon films in such a nonequilibrium way can yield an increase in the boron concentration and thus a larger T_c, as was demonstrated in the case of boron-doped diamond[14–16].

Discussion

In summary, we have shown by *ab initio* calculations that hole-doped sp^3-bonded covalent hydrocarbon K_4-CH is a promising candidate for showing high-T_c superconductivity mediated by the electron-phonon coupling. The key advantages of this system lie in its quickly rising electronic DOS upon doping, together with the presence of high-frequency optical bond-stretching phonon modes and their strong coupling to the holes in the σ-band valence states. At the experimentally accessible doping range of up to 5%[16], T_c in crystalline hydrocarbon K_4-CH can reach 80 K. Our results identify a new carbon-based covalent metal as extraordinary electron-phonon superconductor, and the insights offered by the calculated structural, phonon, and electronic properties lay the foundation for further exploration of this material.

Methods

The calculations are performed using the density functional theory within the local density approximation (LDA)[34, 35], as implemented in the Quantum ESPRESSO code[36]. Norm-conserving pseudopotentials[37] are adopted with a plane-wave cutoff energy of 100 Ry. We employ the virtual crystal approximation[18] to simulate the hole doping by generating B_xC_{1-x} pseudopotentials with $x = 0.01–0.08$. Its feasibility was proved by comparing the electronic structure with the supercell model explicitly including the boron atoms (see Fig. S1 in Supplementary Information). The dynamical matrices and the electron-phonon coupling (EPC) are calculated using the density functional perturbation theory[38]. The phonon dispersion is obtained by the Fourier interpolation of the dynamical matrices computed on a $N_q = 6 \times 6 \times 6$ **q**-mesh. For the electronic integration in the phonon calculation, we use a $N_k = 12 \times 12 \times 12$ **k**-mesh and a Methfessel-Paxton[39] smearing of 0.02 Ry. A finer $N_k = 24 \times 24 \times 24$ **k**-mesh is used for obtaining the EPC and the electronic DOS. Such samplings ensure good convergence of phonon frequencies and the average coupling λ. We have also used the generalized gradient approximation (GGA)[40] for electron-phonon calculations to confirm our results for superconductivity in the hole-doped hydrocarbon (see Table S1 in Supplementary Information).

References

1. Crespi, V. H. Superconductors: Clathrates join the covalent club. *Nature Mater.* **2**, 650–651, doi:10.1038/nmat990 (2003).
2. Blase, X., Bustarret, E., Chapelier, C., Klein, T. & Marcenat, C. Superconducting group-IV semiconductors. *Nature Mater.* **8**, 375–382, doi:10.1038/nmat2425 (2009).
3. Duan, D. *et al.* Pressure-induced metallization of dense $(H_2S)_2H_2$ with high-T_c superconductivity. *Sci: Rep.* **4**, 6968, doi:10.1038/srep06968 (2014).
4. Drozdov, A. P., Eremets, M. I., Troyan, I. A., Ksenofontov, V. & Shylin, S. I. Conventional superconductivity at 203 kelvin at high pressures in the sulfur hydride system. *Nature* **525**, 73–76, doi:10.1038/nature14964 (2015).
5. Kubozono, Y. *et al.* Metal-intercalated aromatic hydrocarbons: a new class of carbon-based superconductors. *Phys. Chem. Chem. Phys.* **13**, 16476–16493, doi:10.1039/c1cp20961b (2011).
6. Weller, T., Ellerby, E. M., Saxena, S. S., Smith, R. P. & Skipper, N. T. Superconductivity in the intercalated graphite compounds C_6Yb and C_6Ca. *Nature Phys.* **1**, 39–41, doi:10.1038/nphys0010 (2005).
7. Emery, N. *et al.* Superconductivity of bulk CaC_6. *Phys. Rev. Lett.* **95**, 087003, doi:10.1103/PhysRevLett.95.087003 (2005).
8. Tanigaki, K. *et al.* Superconductivity at 33 K in $Cs_xRb_yC_{60}$. *Nature* **352**, 222–223, doi:10.1038/352222a0 (1991).
9. Palstra, T. *et al.* Superconductivity at 40 K in cesium doped C_{60}. *Solid State Commun.* **93**, 327–330, doi:10.1016/0038-1098(94)00787-X (1995).
10. Mitsuhashi, R. *et al.* Superconductivity in alkali-metal-doped picene. *Diamond Relat. Mater.* **464**, 76–79, doi:10.1038/nature08859 (2010).
11. Sidorov, V. A. & Ekimov, E. A. Superconductivity in diamond. *Diamond Relat. Mater.* **19**, 351–357, doi:10.1016/j.diamond.2009.12.002 (2010).
12. Nagamatsu, J., Nakagawa, N., Muranaka, T., Zenitani, Y. & Akimitsu, J. Superconductivity at 39 K in magnesium diboride. *Nature* **410**, 63–64, doi:10.1038/35065039 (2001).
13. Kong, Y., Dolgov, O. V., Jepsen, O. & Andersen, O. K. Electron-phonon interaction in the normal and superconducting states of MgB_2. *Phys. Rev.* **64**, 020501, doi:10.1103/PhysRevB.64.020501 (2001).
14. Ekimov, E. A. *et al.* Superconductivity in diamond. *Nature* **428**, 542–545, doi:10.1038/nature02449 (2004).
15. Ishizaka, K. *et al.* Temperature-Dependent Localized Excitations of Doped Carriers in Superconducting Diamond. *Phys. Rev. Lett.* **100**, 166402, doi:10.1103/PhysRevLett.100.166402 (2008).
16. Takano, Y. *et al.* Superconducting properties of homoepitaxial CVD diamond. *Diamond Relat. Mater.* **16**, 911–914, doi:10.1016/j.diamond.2007.01.027 (2007).
17. Bardeen, J., Cooper, L. N. & Schrieffer, J. R. Theory of Superconductivity. *Phys. Rev.* **108**, 1175–1204, doi:10.1103/PhysRev.108.1175 (1957).
18. Boeri, L., Kortus, J. & Andersen, O. K. Three-Dimensional MgB_2-Type Superconductivity in Hole-Doped Diamond. *Phys. Rev. Lett.* **93**, 237002, doi:10.1103/PhysRevLett.93.237002 (2004).
19. Moussa, J. E. & Cohen, M. L. Constraints on T_c for superconductivity in heavily boron-doped diamond. *Phys. Rev.* **77**, 064518, doi:10.1103/PhysRevB.77.064518 (2008).

20. Bourgeois, E., Bustarret, E., Achatz, P., Omnès, F. & Blase, X. Impurity dimers in superconducting B-doped diamond: Experiment and first-principles calculations. *Phys. Rev.* **74**, 094509, doi:10.1103/PhysRevB.74.094509 (2006).
21. Zipoli, F., Bernasconi, M. & Benedek, G. Electron-phonon coupling in halogen-doped carbon clathrates from first principles. *Phys. Rev. B* **74**, 205408, doi:10.1103/PhysRevB.74.205408 (2006).
22. Savini, G., Ferrari, A. C. & Giustino, F. First-Principles Prediction of Doped Graphane as a High-Temperature Electron-Phonon Superconductor. *Phys. Rev. Lett.* **105**, 037002, doi:10.1103/PhysRevLett.105.037002 (2010).
23. Lian, C. S., Wang, X. Q. & Wang, J. T. Hydrogenated K_4 carbon: A new stable cubic gauche structure of carbon hydride. *J. Chem. Phys.* **138**, 024702, doi:10.1063/1.4773584 (2013).
24. Itoh, M. *et al*. New metallic carbon crystal. *Phys. Rev. Lett.* **102**, 055703, doi:10.1103/PhysRevLett.102.055703 (2009).
25. Grimvall, G. The Electron-Phonon Interaction in Metals. (North-Holland, New York, 1981).
26. Allen, P. B. & Dynes, R. C. Transition temperature of strong-coupled superconductors reanalyzed. *Phys. Rev. B* **12**, 905–922, doi:10.1103/PhysRevB.12.905 (1975).
27. Xiang, H. J., Li, Z. Y., Yang, J. L., Hou, J. G. & Zhu, Q. S. Electron-phonon coupling in a boron-doped diamond superconductor. *Phys. Rev. B* **70**, 212504, doi:10.1103/PhysRevB.70.212504 (2004).
28. Calandra, M. & Mauri, F. Theoretical Explanation of Superconductivity in C_6Ca. *Phys. Rev. Lett.* **95**, 237002, doi:10.1103/PhysRevLett.95.237002 (2005).
29. Iyakutti, K., Bodapati, A., Peng, X., Keblinski, P. & Nayak, S. K. Electronic band structure, electron-phonon interaction, and superconductivity of (5,5), (10,10), and (5,0) carbon nanotubes. *Phys. Rev. B* **73**, 035413, doi:10.1103/PhysRevB.73.035413 (2006).
30. Ceppatelli, M., Santoro, M., Bini, R. & Schettino, V. Fourier transform infrared study of the pressure and laser induced polymerization of solid acetylene. *J. Chem. Phys.* **113**, 5991–6000, doi:10.1063/1.1288800 (2000).
31. Cansell, F., Fabre, D. & Petitet, J. P. Phase transitions and chemical transformations of benzene up to 550 °C and 30 GPa. *J. Chem. Phys.* **99**, 7300–7304 (1993).
32. Robertson, J. Diamond-like amorphous carbon. *Mater. Sci. Eng. R.* **37**, 129–281, doi:10.1016/S0927-796X(02)00005-0 (2002).
33. Casiraghi, C., Piazza, F., Ferrari, A. C., Grambole, D. & Robertson, J. Bonding in hydrogenated diamond-like carbon by Raman spectroscopy. *Diamond Relat. Mater.* **14**, 1098–1102, doi:10.1016/j.diamond.2004.10.030 (2005).
34. Ceperley, D. M. & Alder, B. J. Ground State of the Electron Gas by a Stochastic Method. *Phys. Rev. Lett.* **45**, 566–569, doi:10.1103/PhysRevLett.45.566 (1980).
35. Perdew, J. P. & Zunger, A. Self-interaction correction to density-functional approximations for many-electron systems. *Phys. Rev. B* **23**, 5048–5079, doi:10.1103/PhysRevB.23.5048 (1981).
36. Giannozzi, P. *et al*. Quantum ESPRESSO: a modular and open-source software project for quantum simulations of materials. *J. Phys. Condens. Matter* **21**, 395502, doi:10.1088/0953-8984/21/39/395502 (2009).
37. Troullier, N. & Martins, J. L. Efficient pseudopotentials for plane-wave calculations. *Phys. Rev. B* **43**, 1993–2006, doi:10.1103/PhysRevB.43.1993 (1991).
38. Baroni, S., Gironcoli, S., de Corso, A. D. & Giannozzi, P. Phonons and related crystal properties from density-functional perturbation theory. *Rev. Mod. Phys.* **73**, 515–562, doi:10.1103/RevModPhys.73.515 (2001).
39. Methfessel, M. & Paxton, A. T. High-precision sampling for Brillouinzone integration in metals. *Phys. Rev. B* **40**, 3616–3621, doi:10.1103/PhysRevB.40.3616 (1989).
40. Perdew, J. P., Burke, K. & Ernzerhof, M. Generalized Gradient Approximation Made Simple. *Phys. Rev. B Lett.* **77**, 3865–3868, doi:10.1103/PhysRevLett.77.3865 (1996).

Acknowledgements

This study was supported by the National Natural Science Foundation of China (Grants Nos 11274356 and 11674364) and the Strategic Priority Research Program of the Chinese Academy of Sciences (Grant No. XDB07000000). C.F.C. acknowledges support by the US Department of Energy under Cooperative Agreement DE-NA0001982. W.H.D. acknowledges support by the Ministry of Science and Technology of China (Grant No. 2016YFA0301001).

Author Contributions

C.S.L., J.T.W., W.H.D. and C.F.C. designed the study and wrote the paper; C.S.L. carried out *ab initio* simulations. All authors discussed the results and contributed to the manuscript.

Additional Information

Supplementary information accompanies this paper at doi:10.1038/s41598-017-01541-6

Competing Interests: The authors declare that they have no competing interests.

Publisher's note: Springer Nature remains neutral with regard to jurisdictional claims in published maps and institutional affiliations.

Open Access This article is licensed under a Creative Commons Attribution 4.0 International License, which permits use, sharing, adaptation, distribution and reproduction in any medium or format, as long as you give appropriate credit to the original author(s) and the source, provide a link to the Creative Commons license, and indicate if changes were made. The images or other third party material in this article are included in the article's Creative Commons license, unless indicated otherwise in a credit line to the material. If material is not included in the article's Creative Commons license and your intended use is not permitted by statutory regulation or exceeds the permitted use, you will need to obtain permission directly from the copyright holder. To view a copy of this license, visit http://creativecommons.org/licenses/by/4.0/.

© The Author(s) 2017